

Nanomechanical structures with 91 MHz resonance frequency fabricated by local deposition and dry etching

G. M. Kim^{a)}

Microsystems Laboratory, Institute for Microelectronics and Microsystems, Swiss Federal Institute of Technology Lausanne (EPFL), Lausanne, Switzerland

S. Kawai, M. Nagashio, and H. Kawakatsu

Institute of Industrial Science, University of Tokyo, Tokyo, Japan

J. Brugger

Microsystems Laboratory, Institute for Microelectronics and Microsystems, Swiss Federal Institute of Technology Lausanne (EPFL), Lausanne, Switzerland

(Received 24 February 2004; accepted 22 April 2004; published 30 June 2004)

We report an all-dry, two-step, surface nanoengineering method to fabricate nanomechanical elements without photolithography. It is based on the local deposition through a nanostencil of a well-defined aluminum pattern onto a silicon/silicon-nitride substrate, followed by plasma etching to release the structures. The suspended 100-nm-wide, 2- μm -long, and 300-nm-thick nanolevers and nanobridges have natural resonance frequencies of 50 and 91 MHz, respectively. The fabrication method is scalable to a full wafer and allows for a variety of materials to be structured on arbitrary surfaces, thus opening new types of nanoscale mechanical systems. © 2004 American Vacuum Society. [DOI: 10.1116/1.1761240]

I. INTRODUCTION

Nanoelectromechanical systems (NEMS) have recently attracted increased interest as miniaturized force-sensing and resonating devices because they combine simultaneously low force constants ($k < 1 \text{ N/m}$) and ultrafast resonance frequencies ($f > 1 \text{ MHz}$).^{1,2} High-speed atomic force microscopy (AFM)³ and mass-sensitive resonating sensors⁴ are two potential applications. For a rectangular cantilever of spring constant k and mass m , the vacuum resonance frequency is given by

$$f = \frac{1}{2\pi} \sqrt{\frac{k}{(0.24)m}}$$

The only way to increase the resonance frequency without raising the spring constant is to lower the cantilever mass m by further downscaling the device into the submicron regime.

Currently, a typical surface fabrication process to create freestanding elements for microelectromechanical systems involves a multitude of manufacturing steps based on integrated circuit (IC) processing methods including photolithography with “deposition-pattern-etching” cycles and associated substeps. Sacrificial layer etching is typically used to release the structure. In particular, special care is required during the final etching step to avoid surface-tension-related sticking of the nanostructures upon release. Electron-beam exposure can be used to define the layout for freestanding structures at the 100-nm-length scale.^{5,6} However, photolithography-based methods are limited to a specific class of surfaces and materials that can be selectively struc-

tured by the pattern transfer. Other alternative methods to fabricate NEMS reported included the local gallium (Ga^+) doping of silicon by a focused ion beam (FIB) in combination with selective wet etching using potassium hydroxide to fabricate three-dimensional suspended submicron structures,⁷ or scanning methods such as the local oxidation of aluminum by direct laser writing or scanned probes to form an aluminum dioxide etch mask⁸ followed by underetching. Such methods are very useful for the rapid prototyping of NEMS structures, but cannot be used as a cost-efficient manufacturing process.

In this article, we describe the use of a direct nanopatterning method to fabricate suspended nanomechanical elements in two simple steps without the need for photolithography. It is based on the local deposition of a controlled amount of material through the apertures of a miniature shadow mask or nanostencil.^{9–11} Patterns ranging from sub-100 nm and $>100 \mu\text{m}$ can be defined simultaneously in a single-step deposition allowing the structure sizes to span over multiple-length scales. This is important when aiming to form interconnects between nanoscale objects and microdevices. The technique also permits patterning materials on unconventional surfaces because no wet chemistry step is required. It is contact free; hence, it reduces the risk of chemical cross contamination or mechanical surface damage.

II. FABRICATION

A. Nanostencil fabrication

For the current experiments, we fabricated nanostencils by means of a silicon micromachining process to be used as a template for NEMS fabrication. A 500-nm-thick layer of low-stress SiN was deposited by low-pressure chemical vapor deposition onto a double-side polished 380- μm -thick

^{a)}Author to whom correspondence should be addressed; electronic mail: gyuman.kim@knu.ac.kr. Present address: School of Mechanical Engineering, Kyungpook National University, Daegu 702-701, South Korea.

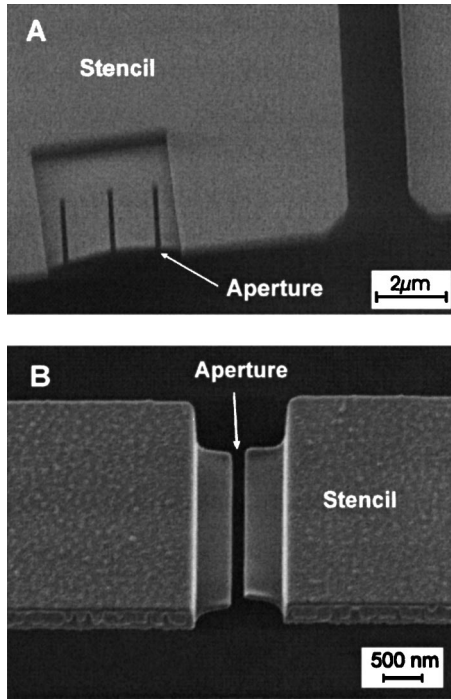


FIG. 1. Microscopic images of micro- and nanoscale apertures made in stencil membrane. (a) Stencil designed for nanocantilever. (b) Stencil designed for nanobridge (double-clamped beam). Local thin membrane and nanoscale apertures connected to microscale apertures were made by FIB milling.

100-mm-size silicon wafer. The internal tensile stress of the SiN layer is about 200 MPa. Optical photolithography (contact mask aligner) was used to define μm -scale patterns in a photoresist, which were subsequently transferred into the topside SiN layer by means of inductively coupled plasma (ICP) etching (C_2F_6 , 20 sccm, 20 °C, 1800 W). Then, the reverse-side SiN was structured in the same way to form the etch mask for a subsequent wafer through-etching using potassium hydroxide (KOH, 40 wt %, 60 °C). This step delineates chips $15 \times 15 \text{ mm}^2$ in size, each containing 16 suspended perforated membranes $2 \times 2 \text{ mm}^2$ in size. For the current experiments, submicron apertures were fabricated by means of a FIB (Ga ions, $0.1 \text{ nC}/\mu\text{m}^2$ at 0.2 pA, 50 kV).¹² For that purpose, the dielectric SiN membrane was coated with a 5-nm-thick conductive gold layer in order to stabilize the ion beam. To facilitate the opening of 100-nm-wide apertures and keep the aspect ratio favorable for shadow evaporation, the SiN membrane was first locally thinned down from 500 to 50 nm. Figure 1 shows parts of the nanostencil after preparation by FIB. Figure 1(a) shows three 170-nm-wide slit apertures in the membrane used to locally deposit the metal mask layout for fabrication of three single-side clamped cantilevers, Figure 1(b) shows a 120-nm-wide aperture for a double-clamped nanobridge.

B. Nanostructure fabrication

The nanostencil was then used as a miniature shadow mask to create the mask pattern for the NEMS, as shown in Fig. 2. The chip containing the nanostencil was positioned

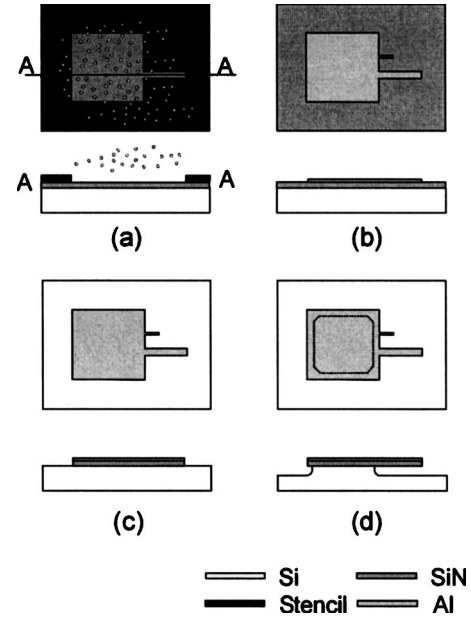


FIG. 2. Schematic view of process step. (a) Local deposition of metal through micro/nanostencil. (b) Remaining metal layer after stencil removal. (c) Pattern transfer into sublayer of SiN using anisotropic ICP etching. (d) Dry releasing of suspended nanomechanical structures by isotropic etching of Si substrate.

and mechanically fixed with a tape on a Si wafer covered with a 200-nm-thick SiN layer. Then, a 100-nm-thick Al material layer was shadow-evaporated via the apertures in the nanostencil onto the SiN layer by means of thermal evaporation (e-beam, base chamber pressure 5×10^{-7} mbar). After removing the nanostencil, the nanostructures on the surface represent a copy of the aperture pattern in the membrane. The Al film forms an effective etch mask in a subsequent pattern transfer etch step into the underlying SiN and sacrificial Si layer. For this purpose, we used anisotropic dry etching with an ICP (C_2F_6 20 sccm, 20 °C, 1800 W) for the SiN, and an isotropic etching by a second ICP etch process (SF_6 20 sccm, 20 °C, 800 W) for the under-etching of the Si and release of the Al/SiN structure. The resulting suspended nanolevers (170 nm wide and $2 \mu\text{m}$ long) and nanobridge (120 nm wide and $2.75 \mu\text{m}$ long) are shown in the scanning electron microscope (SEM) images in Fig. 3. Both nanomechanical elements are formed by bilayers of 100-nm-thick aluminum and 200-nm-thick silicon nitride. The all-dry process allows the release of the nanostructures without damage or surface-tension-related sticking typically related to wet chemical processes.

III. CHARACTERIZATION AND PERSPECTIVES

A heterodyne laser Doppler interferometer with a carrier frequency of 1.1 GHz¹³ and a wavelength of 632 nm was used to measure the mechanical properties of the submicron-sized structures. Figure 4 depicts the configuration of the apparatus. The probe beam was introduced to the vacuum chamber by a polarization maintaining single-mode optical fiber, then terminated by a collimating lens, a quarter-wave

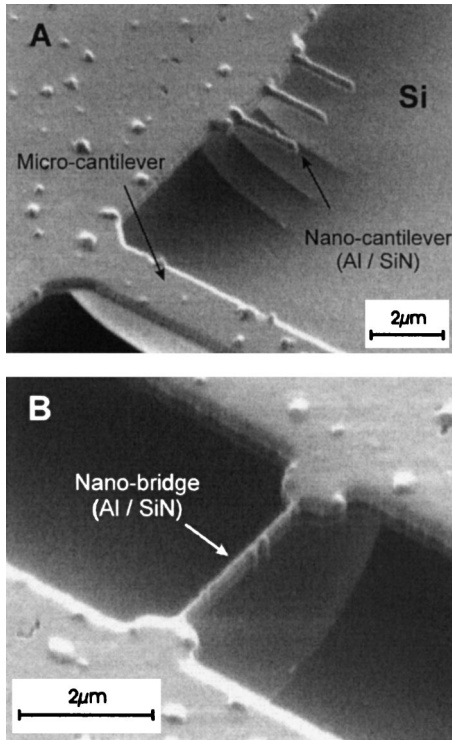


FIG. 3. SEM images of suspended nanomechanical elements: (a) cantilever and (b) double-clamped beam. The nanoscale elemental structures are intrinsically connected with microscale platform.

plate, and a focusing lens. The focal length was 1.6 mm, and the focal diameter 1.2 μm . The samples were excited by photothermal excitation at a wavelength of 780 nm or by a piezo element. A network analyzer was used to sweep the excitation stimulant and to acquire the output of the Doppler interferometer. The velocity measurements of the Doppler interferometer were converted to amplitude of the sample in Figs. 4 and 5.

The three cantilevers of Fig. 3(a) measuring 170(w) \times 300(t) \times 2000(l) nm had natural frequencies in the range of 50 to 67 MHz. The measured Q factors were in the range of 870 to 2500 at 10^{-3} Pa. No surface cleaning or treatment was carried out to improve the Q factor other than air evacuation.

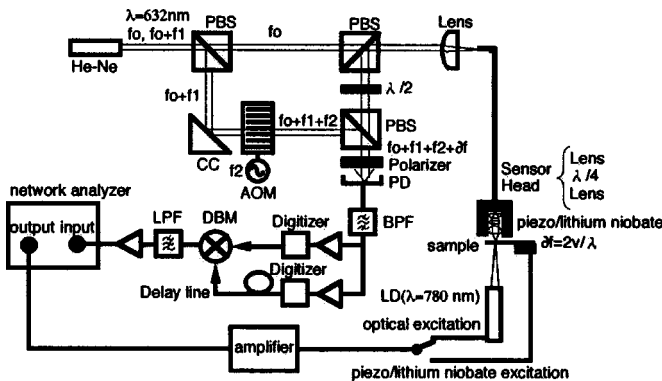


FIG. 4. Heterodyne laser Doppler interferometer with a carrier frequency of 1.1 GHz.

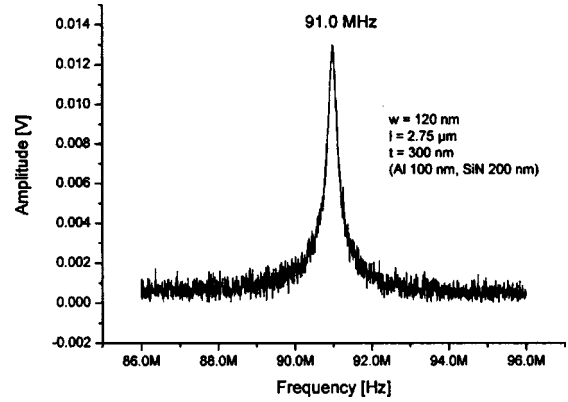


FIG. 5. Measured frequency spectrum of the double-clamped beam shown in Fig. 3(b) with the heterodyne laser Doppler interferometer.

The double-clamped nanobridge shown in Fig. 3(b) measuring 120(w) \times 300(t) \times 2750(l) nm had a measured natural frequency of 91 MHz and a Q factor of 500 at 10^{-3} Pa, shown in Fig. 5.

Depending on the requirements of the final nanostructures, several process combinations of deposition, etching, and releasing may be considered. For example, the structure material can be directly deposited and released, or the etching mask can be deposited on a structural layer followed by etching, mask layer removal, and releasing. Multiple-layer structures including metals, dielectrics, and semiconductors can also be made by multiple deposition and etching. Such multiple-layer structures are expected to find applications as thermally driven nanoscale bimorph elements such as nanogrippers. The method also allows one to reduce the size of piezoelectric sensor and actuator elements for NEMS. The presented single-step deposition method makes the nanopatterning process simple and extremely versatile. For example, sophisticated processes including resist spinning, alignment, exposure, development, metal evaporation, and/or lift-off become obsolete as they can be carried out in one single step using the stencil deposition method.

IV. CONCLUSION

In conclusion, we demonstrated a method of making nanoscale mechanical structures at the length-scale between 120 nm and 2 μm using local deposition through a miniaturized shadow mask and subsequent dry etching. First mechanical characterization using a heterodyne laser Doppler interferometer showed the nanomechanical structures resonate at high natural frequency up to 91 MHz. The proposed method using the stencil is versatile, very simple, and cost effective. These NEMS element structures can be fabricated without costly lithography steps. Moreover, the processes are compatible with standard IC fabrication methods.

ACKNOWLEDGMENTS

The authors are grateful to the Center of Micro/nanofabrication CMI at EPFL at its staff for technical assistance. We acknowledge the financial support of this work by TopNano21 and EPFL.

¹H. G. Craighead, *Science* **290**, 1533 (2000).

²A. N. Cleland and M. L. Roukes, *Nature (London)* **392**, 160 (1998).

³G. T. Paloczi, B. L. Smith, P. K. Hansma, M. A. Wendman, and D. A. Walters, *Appl. Phys. Lett.* **73**, 1658 (1998).

⁴Z. J. Davis, G. Abadal, O. Kuhn, O. Hansen, F. Grey, and A. Boisen, *J. Vac. Sci. Technol. B* **18**, 612 (2000).

⁵D. W. Carr and H. G. Craighead, *J. Vac. Sci. Technol. B* **15**, 2760 (1997).

⁶A. N. Cleland and M. L. Roukes, *Appl. Phys. Lett.* **69**, 2653 (1996).

⁷J. Brugger, G. Beljakovic, M. Despont, N. F. de Rooij, and P. Vettiger, *Microelectron. Eng.* **35**, 401 (1997).

⁸A. Boisen, K. Birkelund, O. Hansen, and F. Grey, *J. Vac. Sci. Technol. B* **16**, 2977 (1998).

⁹M. M. Deshmukh, D. C. Ralph, M. Thomas, and J. Silcox, *Appl. Phys. Lett.* **75**, 1631 (1999).

¹⁰R. Lüthi, R. R. Schlittler, J. Brugger, P. Vettiger, M. E. Welland, and J. K. Gimzewski, *Appl. Phys. Lett.* **75**, 1314 (1999).

¹¹J. Brugger, J. W. Berenschot, S. Kuiper, W. Nijdam, B. Otter, and M. Elwenspoek, *Microelectron. Eng.* **53**, 403 (2000).

¹²G. M. Kim, M. van den Boogaart, and J. Brugger, *Microelectron. Eng.* **67–68**, 609 (2003).

¹³H. Kawakatsu, S. Kawai, D. Saya, M. Nagashio, D. Kobayashi, H. Toshiyoshi, and H. Fujita, *Rev. Sci. Instrum.* **73**, 2317 (2002).